Forschung im Ingenieurwesen (2024)88:5
https://doi.org/10.1007/s10010-024-00726-6

ORIGINALARBEITEN/ORIGINALS

Locally resolved stress measurement in the ultra-hard composites polycrystalline diamond and polycrystalline cubic boron nitride

Bernd Breidenstein[1] · **Nils Vogel**[1]

Received: 30 November 2022 / Accepted: 31 January 2024

Abstract

Cutting tools made of the ultra-hard composites polycrystalline diamond and polycrystalline boron nitride are being used in more and more sectors of machining. Due to the laborious preparation processes such as grinding, brushing, electrical discharge and laser machining, the subsurface of these tools is strongly stressed mechanically and thermally. This also changes the residual stress state in the highly loaded cutting edge area. The measurement of these residual stresses is not possible by established XRD methods due to the highly curved surface of the cutting edge. The measurement method Raman spectroscopy shows high potential for this application, but conversion factors are necessary for the application. These factors enable the conversion of the stress-induced peak shift in the Raman spectrum into absolute residual stress values. Previous conversion factors are mainly based on hydrostatic load cases, which, however, cannot be transferred to the application on cutting tools. In this work, axial load cases were provided by bending and conversion factors were determined by comparing XRD stress measurements and Raman peak shifts. The conversion factors determined were then plotted against existing results from other studies and the causes for the deviations that occurred were determined. By this, for the first time, a conversion factor for an axial load case for cubic boron nitride could be determined and it could be shown that, as for diamond, it differs significantly from the hydrostatic load case.

Ortsaufgelöste Spannungsmessung in den hochharten Kompositmaterialien polykristalliner Diamant und polykristallines kubisches Bornitrid

Zusammenfassung

Zerspanwerkzeuge aus hochharten Schneidstoffen wie polykristalliner Diamant und polykristallinem Bornitrid finden in immer mehr Bereichen der Zerspanung Anwendung. Durch die aufwendigen Präparationsprozesse wie Schleifen, Bürsten, Erodieren und Laserbearbeitung wird die Randzone dieser Werkzeuge mechanisch und thermisch stark beeinflusst. Durch diese Einflüsse wird auch der Eigenspannungszustand im hochbelasteten Schneidkantenbereich verändert. Die Messung dieser Eigenspannungen ist durch etablierte röntgenografische Verfahren aufgrund der stark gekrümmten Oberfläche der Schneidkante nicht möglich. Die Messmethode Raman-Spektroskopie zeigt für diese Anwendung hohes Potential, jedoch sind hierfür Konvertierungsfaktoren notwendig. Diese Faktoren ermöglichen eine Umrechnung des spannungsinduzierten Peakshifts im Raman-Spektrum in absolute Eigenspannungswerte. Bisherige Konvertierungsfaktoren basieren zum großen Teil auf hydrostatischen Lastfällen, die auf die Anwendung an Zerspanwerkzeugen jedoch nicht übertragbar sind. Im Rahmen dieser Arbeit wurden axiale Lastfälle durch eine Biegebelastung bereitgestellt und anschließend die Konvertierungsfaktoren durch die Gegenüberstellung von röntgenografischen Spannungsmessungen und Raman-Messungen ermittelt und mit Literaturwerten verglichen. Dabei konnte erstmals ein Konvertierungsfaktor für einen axialen Lastfall für kubisches Borntitrid ermittelt werden und aufgezeigt werden, dass sich dieser, ebenso wie bei Diamant, stark vom hydrostatischen Lastfall unterscheidet.

✉ Nils Vogel
vogel@ifw.uni-hannover.de

[1] Institute of Production Engineering and Machine Tools, Leibniz Universität, Hannover, An der Universität 2, 30823 Garbsen, Germany

Published online: 11 March 2024

1 Introduction

Ultra-hard cutting materials such as diamond and cubic boron nitride are used in both monocrystalline and polycrystalline states, particularly in manufacturing technology for machining metallic materials like hardened steels or aluminium alloys. In order to produce the tools, tool shaping processes like grinding, brushing, laser or electrical discharge machining are used which mechanically or thermally stress the cutting material and thus strongly influence the subsurface. In addition to topography and microstructure, the residual stress state is highly influenced by tool shaping processes. Furthermore the subsurface of the cutting edge is of major interest due to its high mechanical stressing in the machining process. Topography and microstructure can be reliably determined in this area by optical surface measurement systems or cross-sectional micrographs. The determination of residual stresses in the highly curved area of the cutting edge rounding, which usually has a radius between $r_\beta = 5$ and 100 µm, is not possible with established X-ray-diffraction (XRD) methods, since necessary diffraction conditions are not fulfilled [1]. An alternative method to determine strains and consequently stresses in solids is Raman spectroscopy. By illuminating a solid with monochromatic laser light, a light-matter interaction excites molecular vibrations, which change the wavelength or frequency of the backscattered light. This wavelength change can be observed in the spectrum of backscattered light and quantified by characteristic peaks. The initial light-matter interaction is influenced by interatomic bond lengths which are changed by load or residual stresses. Finally, the described stresses result in a peak shift in the Raman spectrum [2].

Due to the small laser spot diameter of only a few microns, the method enables a spatially resolved analysis in the highly curved area of the cutting edge. The ultra-hard cutting materials polycrystalline diamond (PCD) and polycrystalline cubic boron nitride (PcBN) are both Raman-active, therefore they show an inelastic scattering of the laser-light, and are thus measurable with the described method. Cubic boron nitride exhibits two characteristic peaks at $\omega_{cBN,LO} = 1305\,cm^{-1}$ (longitudinal optical mode) and $\omega_{cBN,TO} = 1054\,cm^{-1}$ (transverse optical mode) when using laser light with a wavelength of $\lambda = 532$ nm [3, 4]. Diamond has a characteristic peak at $\omega_{Dia} = 1332$ cm-1 at the same wavelength [5, 6]. By determining a shift of the characteristic peaks, stresses can be measured close to the surface.

The application for residual stress measurement in nitride-based PVD tool coatings has already been demonstrated extensively [1, 7, 8]. However, there are clear limitations with regard to its validity. In order to determine stresses from the peak shift in the Raman spectrum, a conversion of the peak shift to a residual stress value is necessary. For the high hardness materials diamond and boron nitride this is already known and has been studied in detail [9–12]. The conversion factors were determined by measurements under hydrostatic load in a diamond anvil cell [9, 11]. However, it is noted that the magnitude of the conversion factor C_i for diamond, for example, depends on the type of load. The conversion factor under hydrostatic load differs significantly from the conversion factor under axial load [13]. According to Catledge et al. for a biaxial or a hydrostatic stress condition, the following relationship between biaxial and hydrostatic stress $\sigma_{biaxial}$ / σ_{hydro} and peak shift $\Delta\omega$ is obtained:

$$\sigma_{biaxial} = \frac{\Delta\omega}{C_{biaxial}} \tag{1}$$

$$\sigma_{hydro} = \frac{\Delta\omega}{C_{hydro}} \tag{2}$$

$C_{hydro,Dia}$ here is 2.88 GPa/cm^{-1} and was averaged from existing work in [14] based on the studies from [10–12]. $C_{biaxial,Dia}$ was determined in [14] and is 1.62 GPa/cm^{-1}. Because measurements on the surface of solid bodies generally result in a biaxial stress state at most, it is necessary to determine the conversion factor C under a comparable load. Furthermore, in addition to the cutting materials, the composites PcBN and PCD contain binder phases such as cobalt and tungsten or aluminum, which are not Raman-active in the elemental state, but in some cases form their own spectra in compounds with nitrogen or oxygen. An influence of these elements on the conversion factor is possible.

In this study, the conversion factor C is determined for converting near-surface peak shifts in the Raman spectra of PcBN and PCD under bending stress. For cubic boron nitride (cBN), conversion factors for biaxial or uniaxial loads are not available. Under standard atmospheric conditions, a hydrostatic load on the tool surface, for which a conversion factor exists, is unlikely. Instead, biaxial load cases require specific conversion factors, which can be determined through bending experiments.

2 Experimental details

2.1 Cutting materials

PCD and PcBN cutting materials were used for the investigations. The PCD cutting material has diamond grains with a diameter of $d_g = 4$ µm and a cobalt binder content of 10%. Due to the manufacturing process, the 0.5 mm thick PCD layer is soldered on a 1.1 mm thick tungsten carbide substrate (Data sheet information). The PCD grade is characterized by the good measurability by Raman spectroscopy and the later machining of highly eutectic aluminum alloys

with a high silicon content. Furthermore, a PcBN cutting material with a cBN content of 85% was used, which has an AlWCoB binder and cBN grain diameter of $d_g = 2\,\mu m$ (Data sheet information). The surface exhibits an as-sintered condition, which was prepared using a diamond polishing process for better measurability by Raman spectroscopy. The PcBN grade was selected due to its good machinability by nano- as well as by femtosecond lasers, and will enable near-industrial machining of hardened 100Cr6 in later application tests. Due to the high cBN content, reproducible Raman spectroscopy measurements are possible.

2.2 Four point bending experiment

In order to be able to apply an axial load to the PcBN and PCD cutting materials, a 4-point bending unit was used (Fig. 1). The bending stress is applied by two steel pins which are tensioned by a lever and a screw. To ensure that the stress state remains constant between the stress measurement by XRD and the measurements on the Raman microscope and that a transport-related influence can be excluded, the screw with which the bending force is applied is monitored with a force measuring ring. The measurement takes place exactly in the middle between the two inner contact points. The cutting material specimens had dimensions of $45 \times 6\,mm^2$.

2.3 Residual stress measurement

The XRD residual stress measurements were carried out using the $\sin^2\psi$ method on both cutting materials. A Seifert XRD 3003 ETA five-circle diffractometer from GE Inspection Technologies was used for this purpose. The diffractometer was equipped with a Ketek AXAS-M Silicon Drift Detector (SDD). The point focus of an X-ray tube with Co-anode was used with a point collimator of 2 mm diameter. Both the manufacturing process-induced residual stresses in the unloaded state and the superposition of load and residual stress in the loaded state were determined. For this purpose, the diamond diffraction peak of lattice plane hkl 311 of PCD specimens was evaluated at $2\theta = 112.56°$. For stress measurement of PcBN specimens, the diffraction peak of lattice plane hkl 200 of cubic boron nitride at $2\theta = 59.30°$ was considered.

Table 1 Measurement settings Raman spectroscopy

Parameter	PCD	PcBN
Laserpower P_L	5 mW	10 mW
Accumulation time t	15 s	20 s
Coaddition	2×	

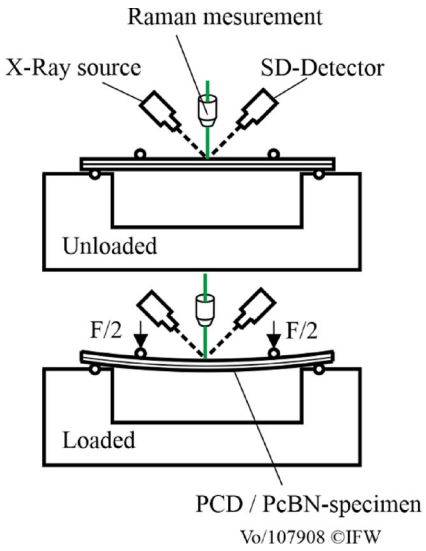

Fig. 1 Setup test bench for applying bending load

2.4 Raman spectroscopy

Raman spectra were recorded using a Bruker Santerra II spectrometer on an Olympus BX51 microscope. A green laser with a wavelength of $\lambda = 532\,nm$ and an objective lens with 100× magnification were used. The measurement settings from Table 1 were used for the measurements. For each load case and cutting material 16 measurements were performed and positioned in the middle of the cutting material segment each offset by 10 µm. (Figure 1). The measuring point diameter d_M was approx. 2 µm.

3 Results

3.1 Residual stress measurement

In order to determine an evaluable peak for the residual stress measurement, an XRD overview diffractogram was recorded for both the PCD and PcBN samples in the first step.

This ensured that the peaks of the carbide substrate, which appear several times below the main cutting material, did not interfere with the evaluated peaks. Interference was also expected from the binder phases cobalt in the PCD cutting material and from tungsten, aluminum and cobalt in the PcBN cutting material.

As the diffractograms in Fig. 2 show, however, no interference can be assumed in the region of the diamond peak 311 and in the region of the boron nitride peak 200, thus enabling a reliable measurement. However, it is also clear that the peaks of the carbide are clearly visible and can be measured for the PCD cutting material. In addition to the

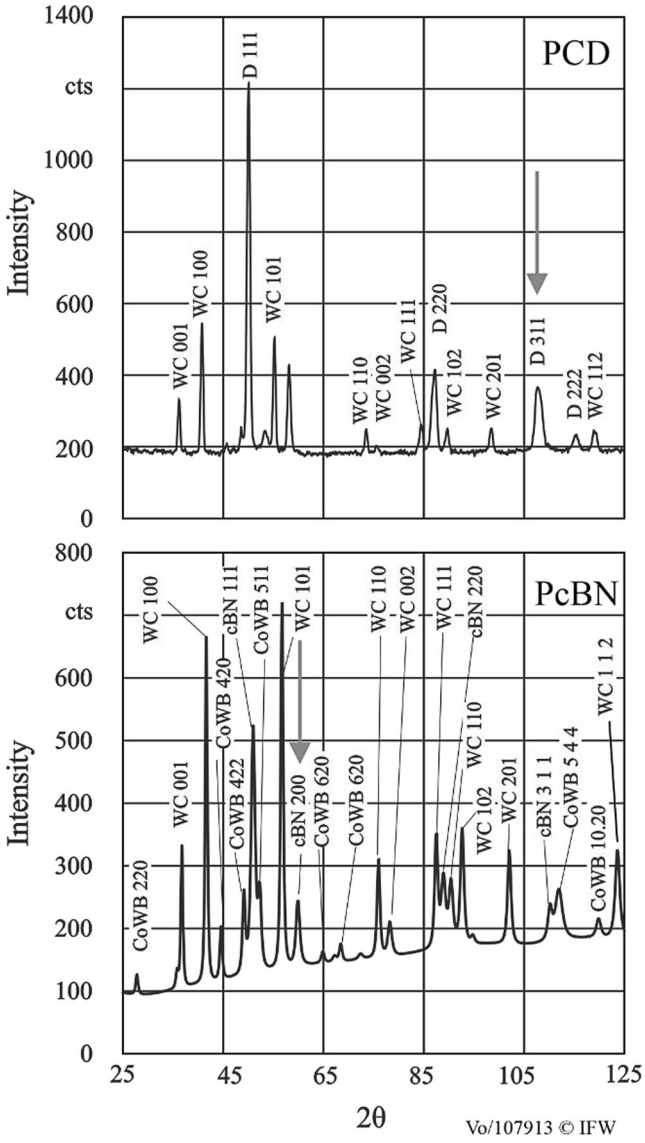

Fig. 2 XRD overview diffractograms (PCD/PcBN)

classical carbide phases, CoW and CoWB are also detected in PcBN.

In the next step, XRD residual stress measurements were carried out on PcBN specimens in the unloaded state. As Fig. 3 shows, the residual stress values parallel to the bending line is $\sigma_{RS,PcBN} = -510$ MPa. In PcBN there is a production-induced compressive residual stress state. The measurement of the PCD specimen shows an initial compressive residual stress state of $\sigma_{RS,PCD} = -1015$ MPa. Thus, initial compressive residual stresses are present in the unloaded state of the ultra-hard material specimens. As shown in Fig. 1, the cutting material specimens were now exposed to a load stress which was kept constant between the XRD measurement and the subsequent Raman measurement. Due to a lever construction required for reasons of limited space, an absolute force in the two upper contact points could

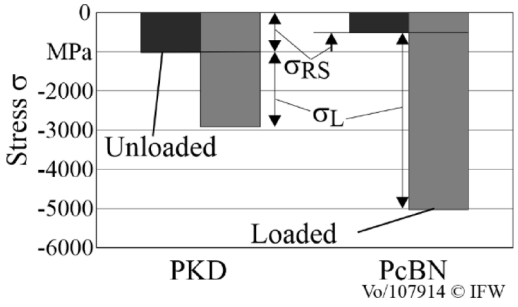

Fig. 3 Load and residual stresses measured by XRD under bending load

not be determined with certainty. The maximum deflection was determined iteratively up to fracture of the specimen and therefore almost corresponds to the maximum possible load that the segment can withstand. The combination of the previously measured residual stresses and the load stresses applied by the bending device is also shown in Fig. 3.

In comparison to the previously measured residual stresses σ_{RS}, the applied load stresses σ_L occur as shown in Fig. 3. For the PcBN cutting material, additional load stresses $\sigma_{L,PcBN} = -4515$ MPa and for the PCD cutting material $\sigma_{L,PCD} = -1900$ MPa occur.

The additionally applied load stresses of 187% for PCD and 870% for PcBN of the original compressive residual stress are significantly higher and suggest a significant peak shift in the Raman spectrum.

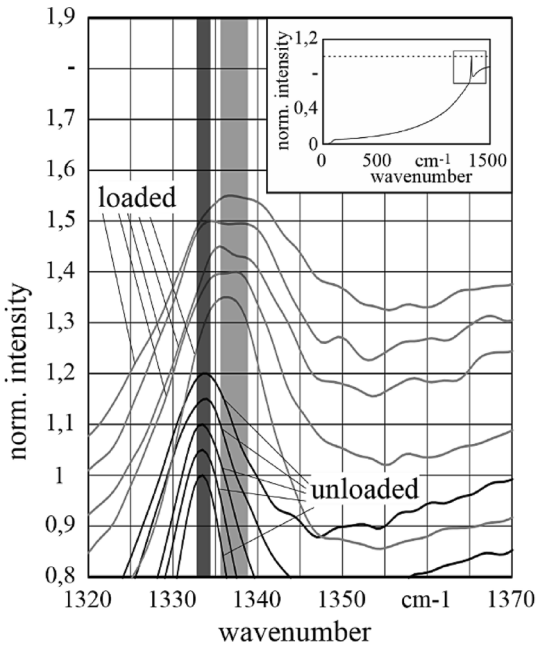

Fig. 4 Peak shift in the Raman spectrum in the loaded and unloaded state (Diamond)

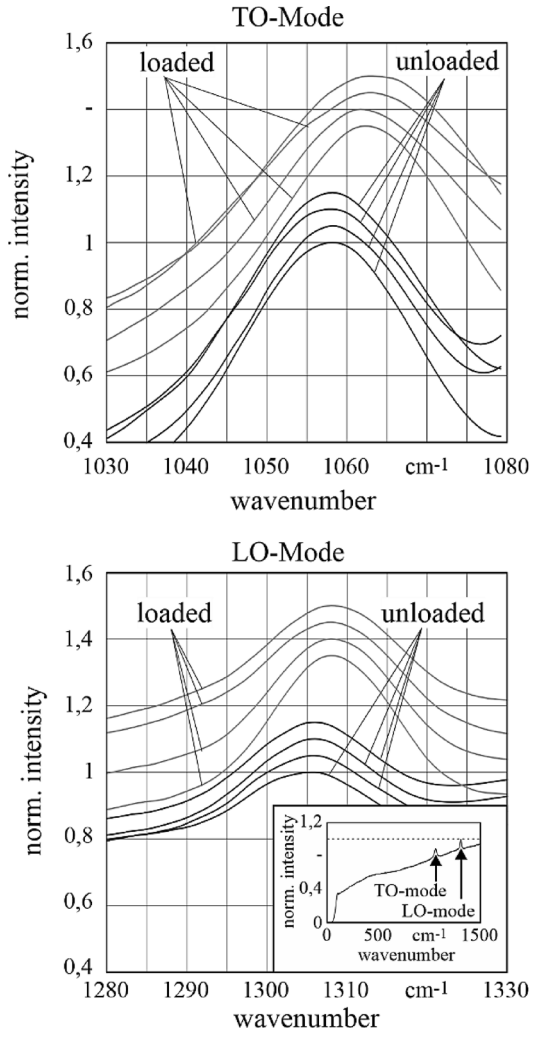

Fig. 5 Peak shift in the Raman spectrum in the loaded and unloaded state (cBN)

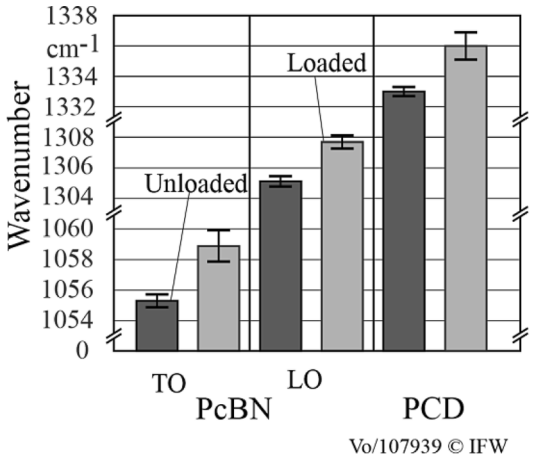

Fig. 6 Fitted peak positions in loaded and unloaded state

3.2 Raman-Spectroscopy

Parallel to the XRD stress measurements, 16 Raman measurements were recorded in the same area on the unloaded and loaded cutting material specimens with an offset of 10 µm. As described above, the peaks at 1050 cm^{-1} (TO mode) and 1305 cm^{-1} (LO mode) for PcBN and 1332 cm^{-1} for PCD were recorded for the load cases described in Sect. 2.1. A corresponding overview is shown in Fig. 4 top and Fig. 5 bottom. Considering the spectra of the unloaded and the loaded PCD samples in Fig. 4, the difference is evident. When a compressive load is applied, there is a clear shift towards higher wavenumbers. Furthermore, there is a broadening of the peak in the loaded condition. In Fig. 4, it should be noted that the spectra were normalized to the highest point and then shifted vertically for a better overview.

If the spectra of the unloaded and loaded PcBN specimens in Fig. 5 are considered, a clear difference also becomes visible. When a compressive load is applied, there is a clear shift towards higher wavenumbers. In particular, for the TO mode, it is a stronger peak shift to higher wavenumbers compared to the LO mode. A clear widening of the peak, as previously seen in the observation of the diamond peak in the PCD cutting material, cannot be seen.

In order to reliably determine the exact position of the peaks in the Raman spectrum, the program Fityk was used and a spline baseline adjustment was performed in the first step [15]. Subsequently, the peak positions in both the cBN and PCD spectra were determined using a Gaussian fit. The determined peak positions are shown for both modes in the PcBN as well as in the diamond spectrum in Fig. 6. They confirm the previous qualitative observation of the peak shift. For both cutting materials, there is a peak shift to higher wavenumbers.

The previously observed higher peak shift of the TO-mode compared to the LO-mode of the PcBN can be confirmed here once again.

In addition to the position of the peaks themselves, a closer look at Fig. 4 shows that the peaks determined in the PCD spectrum broaden under load. To quantify this, the FWHM was determined. The result is shown in Fig. 7 and confirms the subjective broadening of the peaks due to a significantly increased FWHM.

4 Discussion

The results presented show that there is a clear peak shift in both the cBN and diamond spectra at a strong compressive load induced by bending. The two considered load cases can clearly be separated by looking at the peak positions and the peak shift of both cBN and diamond. However,

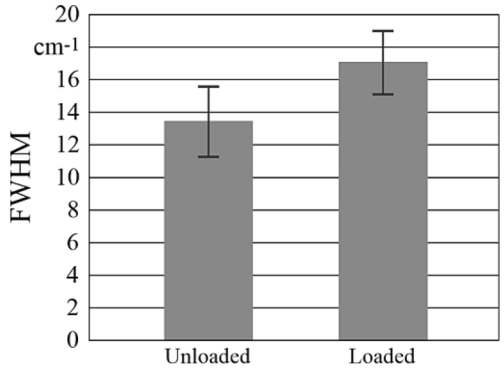

Fig. 7 FWHM in unloaded and loaded state

using comparison values based on existing conversion factors from Sanjurjo et al. shows a significant deviation, as shown in Fig. 7 for PcBN. The conversion factors of Sanjurjo et al. are $C_{cBN.S.LO} = 3.45\,GPa/cm^{-1}$ (LO mode) and $C_{cBN.S.TO} = 3.39\,GPa/cm^{-1}$ (TO mode), respectively. These conversion factors are significantly higher than the resulting conversion factors from this investigation of $C_{cBN.B.LO} = 1.14\,GPa/cm^{-1}$ (LO mode) and $C_{cBN.B.TO} = 1.60\,GPa/cm^{-1}$ (TO mode). However, it is clearly evident that the peak position in the stress-free state, which is obtained both by means of the linear relationship from [9] and by means of extrapolation from the peak positions from Fig. 7 converges closely. The difference here is less than 1.5 wavenumbers for both modes (Fig. 8).

The absolute peak position of a stress-free sample can therefore be reliably determined with the presented method for cBN cutting materials. However, the determination of load or residual stresses does not agree with the literature values.

The linear relationship for hydrostatic loading and for biaxial loading from [14, 16–20] is included for direct comparison. If the determined peak positions are compared with a hydrostatic load case, a strong deviation can be seen. Especially in comparison to the results of Ocelli et al., Mitra et al. and Catledge, a significant difference in the slope of the linear interpolation becomes evident (Fig. 9). As observed, this behavior resembles hydrostatic load stresses in cBN cutting material. It is not possible to compare the presented investigations with investigations that apply the load stresses hydrostatically.

However, in addition to hydrostatic investigations, Catledge et. al. also investigated a biaxial load case in order to analyse the peak shift on diamond coatings. The conversion factor $C_{Dia,C} = 1.62\,GPa/cm^{-1}$ for this load case is significantly lower. If this is compared with the conversion factor $C_{Dia,B} = 1.36\,GPa/cm^{-1}$ determined from the measurement data in this study, there is a significantly higher agreement at high load stresses. However, it is noticeable that the stress-free wavenumber is below $1332\,cm^{-1}$. Adjusting the determined linear interpolation to align with the point $\omega = 1332\,cm^{-1}$, the agreement with findings of Catledge et al. increases.

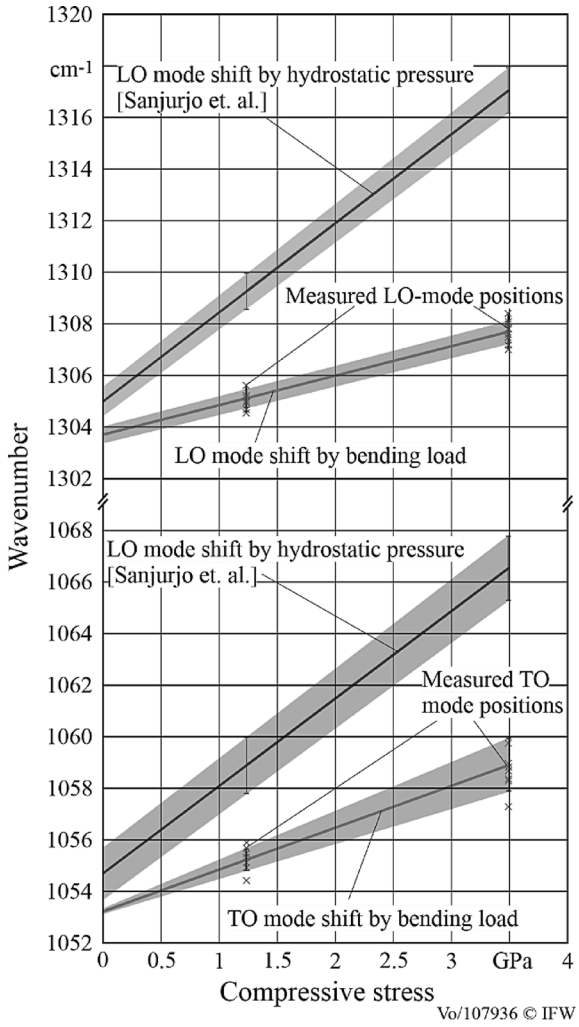

Fig. 8 Peak position as a function of applied compressive bending stresses (PcBN)

Furthermore, there is also close agreement with the values of Ager et al. at low pressures [21]. The load-dependent shift of the split peaks (singlet and doublet) also described by Ager et al., which according to [19, 21] occur at high pressures, exhibits a significantly lower slope (singlet) or higher slope (doublet). The load therefore does not lead to a separation of the peak into singlet and doublet. However, if the FWHM is examined more closely as in Fig. 7, a broadening of the peak can be seen when the load stresses is applied. This indicates that there may already be two peaks that cannot be considered separately. This broadening of the peak due to an applied load stress has also already been demonstrated by Nasdala et al. and Ono et al. [22, 23]. In this context, the peak broadening can be explained by an increase in defects in the diamond under load [23].

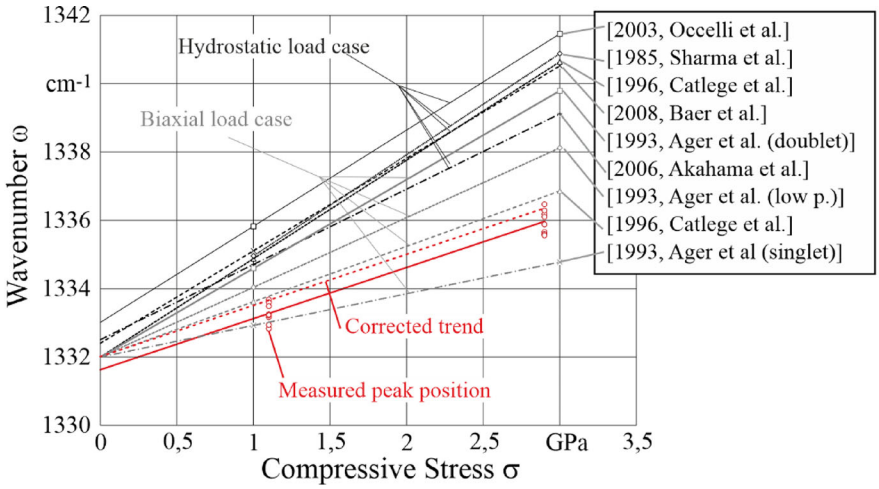

Fig. 9 Peak position as a function of applied compressive bending stresses (PCD)

The strong difference in the peak shift between hydrostatic and axial loading can be explained by the cubic crystal structure of diamond and boron nitride.

According to Angel et al., the relationship between strain or stress and the peak shift is generally given by Eq. 3. In this equation, the wavenumber shift depends on the strain $\epsilon\epsilon$ of the crystal and on the direction-dependent component of the material-dependent Grüneisen tensor γ [2].

$$\frac{-\Delta\omega^m}{\omega_0^m} = \gamma_1^m \varepsilon_1 + \gamma_2^m \varepsilon_2 + \gamma_3^m \varepsilon_3 + \gamma_4^m \varepsilon_4 + \gamma_5^m \varepsilon_5 + \gamma_6^m \varepsilon_6 \quad (3)$$

For triclinic crystal systems, for example, no constraints exist and no simplification can be made. This means that the peak shift is individually dependent on strains/stresses from all directions.

However, for cubic crystals and thus for PCD and PcBN the following can be applied from Angel et al. [2]:

$$\gamma_1^m = \gamma_2^m = \gamma_3^m \quad (4)$$

$$\gamma_4^m = \gamma_5^m = \gamma_6^m = 0 \quad (5)$$

Consequently, the peak shift depends only on the load-induced volume change. Thus, if stresses are applied to the cutting material in all directions due to a hydrostatic load case, a strong load-induced peak shift occurs.

Because of the low information depth of the method, a biaxial residual stress state is assumed here, similar to Spieß et al. as it is for the XRD method [24].

As only loads from two directions influence the volume of the cutting material, the volume change caused by the load is also correspondingly lower. This results in a smaller peak shift. This finding clearly shows the limitation of (residual) stress measurement by Raman spectroscopy on cubic crystalline cutting materials such as PCD and PcBN. Biaxial residual stress states close to the surface can, however, be well described with Raman spectroscopy. For the conversion of peak shifts into residual stresses, the conversion factors $C_{Dia,B}$, $C_{cBN,B,LO}$ and $C_{cBN,B,TO}$ determined in this work are therefore more suitable for both cutting materials than the existing factors from the literature for hydrostatic load cases. This leads to new findings, particularly for cBN, as a biaxial conversion factor was not yet available.

5 Conclusion

The presented results could clearly show that the conversion factor C, which is necessary for (residual) stress measurements by Raman spectroscopy, strongly depends on the induced load case. According to the literature, the coefficients for diamond derived from hydrostatic loads in diamond anvil cells are significantly higher than those for biaxial or monoaxial loads. This can be explained by the influence of the volume change on the peak shift in the Raman spectrum. The determined conversion factor for diamond $C_{Dia,B}$ for a biaxial load case is to be regarded as clearly more suitable, since at the surface a hydrostatic load case is not possible.

The same applies to the previously available conversion factors $C_{cBN,S,LO}$ and $C_{cBN,S,TO}$ for PcBN. The conversion factors valid for hydrostatic load cases differ strongly from the biaxial conversion factors $C_{cBN,B,LO}$ and $C_{cBN,B,TO}$ presented in this work. Since there is no hydrostatic load at the surface of PcBN tools, it can be assumed that the newly determined conversion factors are also better suited for determining residual stresses in cutting tools.

Whether the conversion factors also apply directly to other cutting material grades with lower cutting material content and other binder systems is to be expected due to the same cutting material phase, but it is planned to investigate this in a further bending experiment. In the future, the determined conversion factors will be used to convert the results of Raman measurements on ground and lasered

PcBN and PCD tools into absolute residual stress values. It is then planned to investigate the influence of these residual stress values on tool life of these tools when machining roller bearing steel and silicon-containing hypereutectic aluminium alloys.

Acknowledgements The authors would like to thank the German Research Foundation (DFG) for funding research project BR 2967/22-1 "Influence of preparation-induced residual stresses in the cutting edge of cutting tools on the wear behavior of extremely hard cutting materials." Furthermore, the authors would like to thank the company Element Six for providing the cutting materials.

Funding Open Access funding enabled and organized by Projekt DEAL.

Conflict of interest B. Breidenstein and N. Vogel declare that they have no competing interests.

References

1. Breidenstein B, Vogel N, Behrens H, Dietrich M, Andersson JM (2022) Locally Resolved Residual Stress Measurements in (Al,Ti)N Coatings Using Raman Spectroscopy. Tribol Ind Vol 44(1):143–149. https://doi.org/10.24874/ti.1144.06.21.08
2. Angel RJ, Muri M, Mihailova B, Alvaro M (2019) Stress, strain and Raman shifts. Z Krist 234(2):129–140. https://doi.org/10.1515/zkri-2018-2112
3. Ono S, Mibe K, Hirao N, Ohishi Y (2015) In situ Raman spectroscopy of cubic boron nitride to 90 GPa and 800 K. J Phys Chem Solids 76:120–124. https://doi.org/10.1016/j.jpcs.2014.09.001
4. Herchen H, Cappelli MA (1993) Temperature dependence of the cubic boron nitride Raman lines. Phys Rev B 47:14193. https://doi.org/10.1103/PhysRevB.47.14193
5. Ramaswamy C (1930) Raman Effect in Diamond. Nature 125:704. https://doi.org/10.1038/125704b0
6. Solin SA, Ramdas AK (1970) Raman Spectrum of Diamond. Phys Rev B 1:1687–1698. https://doi.org/10.1103/PhysRevB.1.1687
7. Constable CP (2000) Raman Microscopic Studies of PVD Deposited Hard Ceramic Coatings. Dr Thesis
8. Breidenstein B, Vogel N, Behrens H, Dietrich M, Andersson JM (2022) Determination of Local Residual Stress on Post-Treated TiAlN-Coated Tungsten Carbide Tools. J Surf Investig X-ray Synchrotron Neutron Tech 16(4):663–671. https://doi.org/10.1134/S1027451022040231
9. Sanjurjo JA, Lopez-Cruz E, Vogl P, Cardona M (1983) Dependence on volume of the phonon frequencies and the ir effective charges of several III–V semiconductors. Phys Rev B. https://doi.org/10.1103/PhysRevB.28.4579
10. Mitra SS, Brafman O, Daniels WB, Crawford RK (1969) Pressure-Induced Phonon Frequency Shifts Measured by Raman Scattering. Phys Rev 186(3):942–944. https://doi.org/10.1103/PhysRev.186.942
11. Boppart H, van Straaton J, Silvera IF (1985) Raman spectra of diamond at high pressures. Phys Rev B 32(2):1432–1425. https://doi.org/10.1103/PhysRevB.32.1423
12. Whalley E, Lavergne A, Wong P (1976) Hydrostatic optical cell with glass windows for 25 kilobar. Rev Sci Instrum 47:845–848. https://doi.org/10.1063/1.1134752
13. Catledge SA, Vohra KV (1995) High density plasma processing of diamond films on titanium: Residual stress and adhesion measurements. J Appl Phys 78:7053–7058. https://doi.org/10.1063/1.360409
14. Catledge SA, Vohra KV, Ladi R, Ghanshyam R (1996) Micro-raman stress investigations and X-ray diffraction analysis of polycrystalline diamond (PCD) tools. Diamond and Related Materials 5 1159–1165 https://doi.org/10.1016/0925-9635(96)00534-1
15. Wojdyr M (2010) Fityk: a general-purpose peak fitting program. J Appl Cryst 43(5):1126–1128. https://doi.org/10.1107/S0021889810030499
16. Occelli F, Loubeyre P, LeToullec R (2003) Properties of diamond under hydrostatic pressures up to 140 GPa. Nature Mater 2:151–153. https://doi.org/10.1038/nmat831
17. Sharma SK, Mao HK, Bell PM, Xu JA (1985) Measurement of stress in diamond anvils with micro-Raman spectroscopy. J Raman Spectroscopy 16:350–352
18. Baer JB, Chang ME, Evans WJ (2008) Raman Shift of Stressed Diamond Anvils: Pressure Calibration and Culet Geometry Dependence. J Appl Phys. https://doi.org/10.1063/1.2963360
19. Ager JW III, Drory MD (1993) Quantitative measurement of residual biaxial stress by Raman spectroscopy in diamond grown on a. Ti Alloy By Chem Vap Depos Phys Rev B 48(4):2601–2606
20. Akahama Y, Kawamura H (2005) Raman study on the stress state of [111] diamond anvils at multimegabar pressure. J Appl Phys. https://doi.org/10.1063/1.2115098
21. Ager JW III (1995) Residual stress in diamond and amorphous carbon films. Material Research Society. Proceedings, vol 383. Symposium, pp 143–151 https://doi.org/10.1557/PROC-383-143
22. Nasdala L, Hofmeister W, Harris JW, Glinnemann J (2005) Growth zoning and strain patterns inside diamond crystals as revealed by Raman maps. Am Mineral 90:745–748. https://doi.org/10.2138/am.2005.1690
23. Ono S, Mibe K, Ohishi Y (2014) Raman spectra of culet face of diamond anvils and application as optical pressure sensor to high temperatures. J Appl Phys. https://doi.org/10.1063/1.4891681
24. Spieß L, Teichert G, Schwarzer R, Behnken H, Genzel C (2009) Moderne Röntgenbeugung. Vieweg+Teubner, Wiesbaden